Photoreduction of Methyl Viologen in Zeolite X

Koodali T. Ranjit and Larry Kevan*

Department of Chemistry, University of Houston, Houston, Texas 77204-5003

Received: August 17, 2001; In Final Form: October 27, 2001

The photoreduction of methyl viologen (MV^{2+}) was examined in zeolite X. A series of alkali metal ion-exchanged zeolite X materials with ion-exchanged methyl viologen was photoionized with 320 nm light at room temperature in the absence of any reducing counteranion. Photoreduction of methyl viologen containing alkali metal ion-exchanged zeolite X results in the formation of methyl viologen cation radicals ($MV^{\bullet+}$). The radicals were identified by electron spin resonance (ESR). Upon irradiation at room temperature the samples turn light blue in color and a single line ESR spectrum characteristic of the methyl viologen radical cation is observed. The photoyield depends on the nature of the alkali metal ion-exchanged into the zeolite framework. The photoyield increases in the order $Li-X/MV^{2+} < Na-X/MV^{2+} < K-X/MV^{2+} < Rb-X/MV^{2+} < Cs-X/MV^{2+}$. The donor strength of the zeolite framework increases in the order $Li-X < Na-X < K-X < Rb-X < Cs-X$. Thus, the electron donor is suggested to be the anionic aluminosilicate framework of the host zeolite. This is supported by a linear correlation of the photoyields of alkali metal ions exchanged into zeolite X with Sanderson's partial charges on the framework oxygens.

Introduction

There is considerable interest in the development of artificial photoredox systems.[1−3] One of the main objectives is in maintaining the integrity of the charge separated state long enough so that the free energy can be utilized in driving a chemical reaction. Current research is directed toward the design of efficient photoredox systems that can inhibit back electron transfer. The main problem in achieving such long-lived charge separation is back electron transfer, which is thermodynamically favorable and very rapid. Back electron transfer results in the loss of the potential converted energy into heat.

Many host systems have been examined to improve the efficiency of the energy storage by preventing the back-electron-transfer reaction.[4−6] Heterogeneous systems such as micelles, vesicles, silica gels, and molecular sieves can provide appropriate spatial organization of both the donor and acceptor molecules to retard back electron transfer.[7−10] Thus, appropriate tuning of the electronic and spatial properties of the host system can prevent undesirable back electron transfer.

Dimethyl viologen commonly known as methyl viologen is an efficient electron acceptor for artificial photoredox systems.[11−14] MV^{2+} can be easily reduced by chemical, electrochemical, and photochemical methods.[15−20] However, most of these studies include an added molecular electron donor such as bipyridinium salts or alcohols. The photoreduction of methyl viologen has been studied in vesicular and micellar suspensions.[21−23] This molecule has also been used as an electron acceptor in zeolites.[24−26]

There is considerable interest in the use of microporous materials, such as zeolites, as hosts for photoinduced charge separation. Zeolites have often been the choice because their regular microporous framework provides an opportunity to organize a supramolecular assembly where the different stages of the overall photochemical process (light absorption, energy transfer, and chemical reaction) can take place in a well-defined arrangement.[27,28] The zeolite framework contains pores, channels, and cages that possess an anionic charge. This charge is neutralized by the presence of countercations, often sodium. These cations are easily exchangeable, and hence it is easy to change the donor strength or basicity of the zeolite framework. The cations in zeolites are known to play important chemical roles other than merely compensating the negative charge of the framework.[29−35] Importantly, it has been shown that the cations govern the donor strength of the zeolite framework.[36−40] For example, zeolite Y normally behaves as an acid catalyst in various reactions with Na^+ as the countercation. However, it can be switched to a base catalyst by replacement of Na^+ by Cs^+ cation.[32,34,39,41] Thus, replacement of an alkali metal cation with another can dramatically alter the donor strength of the zeolite framework. The donor strength of the framework has been demonstrated to increase upon increasing the electropositivity of the cation.[42,43] X-ray photoelectron spectroscopy,[44] infrared spectroscopy[45] and ultraviolet spectroscopy[38] have been used to establish this.

The ability of zeolites to accept electrons is well established.[46−48] The structure of the sites responsible for the electron acceptor ability is not established, but it is widely accepted that this property of zeolites is related to the presence of acid centers. In contrast, the reverse situation in which zeolites act as single electron donors is far less well documented.[49−51]

The photoreduction of MV^{2+} in zeolites has been studied by ESR in zeolite X and Y at 77 K by McManus et al.[49] However, no ESR spectrum attributable to the methyl viologen cation radical ($MV^{\bullet+}$) was observed from samples that were irradiated at room temperature. Surprisingly, they also did not observe significant changes in the yield of the photoproduced $MV^{\bullet+}$ by exchanging Na^+ by Li^+, K^+, or Cs^+. In contrast, Alvaro et al. have reported the photolysis of methyl viologen incorporated within zeolites.[50] The yield of $MV^{\bullet+}$ was influenced by the nature of the alkali metal ion-exchanged into zeolite Y. Laser flash photolysis of Li^+, Na^+, and K^+ ion-exchanged into zeolite Y enabled the detection of $MV^{\bullet+}$ as a long-lived transient on the microsecond time scale. For Rb^+ and Cs^+ ion-exchanged into zeolite Y, the photogenerated $MV^{\bullet+}$ was found to be long-

10.1021/jp013194t CCC: $22.00
Published on Web 01/04/2002

lived and could be detected by conventional diffuse reflectance spectroscopy. Yoon et al.[51] were able to detect $MV^{\bullet+}$ from MV^{2+}−arene donor charge-transfer complexes in M−X (M = Cs^+, Rb^+, K^+) zeolites. $MV^{\bullet+}$ did not occur in the complete absence of any arene donor. In view of these conflicting reports, it is important to restudy the photoreduction of MV^{2+} in alkali metal ion-exchanged zeolites.

ESR provides a convenient technique to monitor the formation of any photoproduced $MV^{\bullet+}$. We have been able to detect $MV^{\bullet+}$ by ESR in Li^+, Na^+, K^+, Rb^+, and Cs^+ ion-exchanged zeolite X with incorporated MV^{2+}, denoted as M−X/MV^{2+}, at room temperature. The aim of the present study was to obtain experimental evidence that zeolites can act as single electron donors and to establish a semiquantitative relationship between the physicochemical parameters of the zeolites and their ability to act as electron donors. A relatively high photoyield and excellent stability was observed in Cs^+ ion-exchanged zeolite X, which suggests that such systems can act as potential candidates for photochemical conversion and storage devices. The photoyield was found to increase in the order H−X/MV^{2+} < Li−X/MV^{2+} < Na−X/MV^{2+} < K−X/MV^{2+} < Rb−X/MV^{2+} < Cs−X/MV^{2+}. The donor strength of the zeolite framework increases in the order Li−X < Na−X < K−X < Rb−X < Cs−X. Thus, we have been able to show that the basicity of the framework strongly influences the electron donor ability of zeolite X.

Experimental Section

Preparation of Zeolite M−X. Na−X (Grace Division Chemicals) and Na−A (Union Carbide) zeolite were commercial samples and used as received. The alkali metal ions were incorporated into the zeolite materials in extraframework positions by liquid-state ion exchange. Typical liquid-state ion exchange was performed by adding 20 mL of 5×10^{-1} M $LiNO_3$, KNO_3, $RbNO_3$, or $CsNO_3$ to 2 g of Na−X zeolite and the mixture stirred overnight at room temperature. The excess liquid was decanted off and another 20 mL of the stock alkali metal salt solution added. Once again this mixture was stirred overnight at room temperature. This procedure was repeated four times for each zeolite. The samples were then centrifuged, washed with hot distilled water to remove any excess metal ions on the surface, and then dried in air to form M−X samples. Zeolite H−X was prepared by exchanging Na^+ with NH_4^+ four times followed by calcination, as reported in the literature.[52] For ESR measurements, 0.1 g of the sample was transferred into Suprasil quartz tubes (30 cm × 3 mm o.d.), which were sealed at one end. About 1 cm of glass wool was placed in the quartz tube above the zeolite sample. The quartz tube was attached to a vacuum line and evacuated at 100 ± 5 °C for 36 h to remove traces of oxygen and water. The tube was then removed and flame sealed.

Methyl Viologen Incorporation. A stock 0.1 M solution of dimethyl viologen dichloride (Aldrich Chemical Co.) was prepared in deionized water and purged with nitrogen gas for 1 h. Methyl viologen was exchanged into the zeolite by placing 0.1 g of the alkali metal ion-exchanged zeolite into 1 mL of the stock methyl viologen solution contained in a centrifuge tube. This mixture was then placed in an oven at 70 ± 4 °C for 14 h. Following exchange, the centrifuge tube was placed into an IEC centrifuge unit and the mixture spun at 700 rpm for 10 min. After centrifugation, the excess liquid was carefully decanted. The zeolite was then washed with 5 mL of hot deionized water. This dispersion was agitated and subjected to a further 10 min of centrifugation. The zeolite was washed four times in this way. All the MV^{2+} ion-exchanged zeolite X were dried in air at 80 ± 6 °C and are denoted as M−X/MV^{2+}, where M is an alkali metal ion.

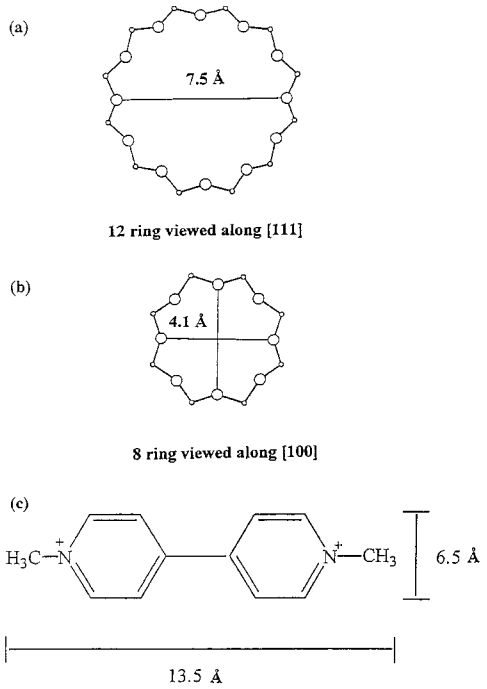

Figure 1. (a) Basic structural unit of zeolite X. (b) Basic structural unit of zeolite A. (c) Molecular dimensions of methyl viologen molecule.

Characterization. X-ray diffraction patterns were recorded on a Siemens 5000 X-ray diffractometer using Cu Kα radiation of wavelength 1.541 Å in the range $10° < 2\theta < 50°$. Chemical analysis was performed by electron microprobe analysis on a JEOL JXA-8600 spectrometer. The composition of the alkali metal ion-exchanged zeolite was determined by calibration with known standards and by averaging over several defocused areas to give the bulk composition. ESR spectra were recorded at room temperature at 9.5 GHz using a Bruker ESP 300 spectrometer with 100 kHz field modulation and low microwave power to avoid power saturation. Photoproduced methyl viologen radical cation ($MV^{\bullet+}$) yields were determined by double integration of the ESR spectra using the ESP 300 software. Each photoyield is an average of three scans and has a precision of less than 4%. Thermal gravimetric analysis (TGA) of the samples was performed using a TGA 2050 analyzer from TA instruments in an oxygen atmosphere at a heating rate of 10 °C/min.

Photoirradiation. The methyl viologen containing zeolite materials were irradiated using a 300 W Cermax xenon lamp (ILC-LX 300 UV) at room temperature. The incoming light was passed through a 10 cm water filter to prevent infrared radiation and through a Corning No. 7-54 with 90% transparency from 240 to 400 nm with a maximum wavelength at 320 ± 20 nm. The samples were placed in a quartz Dewar and rotated at 4 rpm to ensure even irradiation. The photoproduced methyl viologen cation radicals were identified by ESR.

Results

The basic structural units of zeolites X and A are shown in Figure 1. Using a space-filling model based on the covalent radii of the constituent atoms; the dimensions of methyl viologen are 13.5 × 6.5 × 3.5 Å. The cage structure of zeolite X can be described as assembled from sodalite cages linked by double

TABLE 1: Chemical Composition of the Alkali Metal Ion-Exchanged Zeolite X

zeolite	unit cell composition
Cs−X	$Cs_{24}Na_{30}Al_{54}Si_{138}O_{384}$
Rb−X	$Rb_{24}Na_{30}Al_{54}Si_{138}O_{384}$
K−X	$K_{24}Na_{30}Al_{54}Si_{138}O_{384}$
Na−X	$Na_{54}Al_{54}Si_{138}O_{384}$
H−X	$H_{30}Na_{24}Al_{54}Si_{138}O_{384}$

six rings of oxygen bridged tetrahedra thus producing large 13 Å super cages connected by 12-ring windows with openings 7.5 Å in diameter. Thus it is possible to incorporate a methyl viologen molecule into zeolite X. The X-ray diffraction patterns of Na−X, Na−A, and other alkali metal ion-exchanged zeolites reveal them to be highly crystalline, and the XRD patterns agree well with the literature data.

The chemical compositions of the alkali metal ion-exchanged zeolite X materials used are given in Table 1. Despite repetition of the exchange procedure four times, the elemental analyses of the final exchanged zeolites revealed incomplete exchange of the Na^+ ion. The Li−X sample could not be analyzed due to the instrumental limitation in detecting light elements. However, we expect the Li concentration in Li−X to be similar to other alkali metal ion concentrations in zeolites M−X since the ion-exchange procedures were carried out under identical conditions.

The photoexcitation of methyl viologen is extremely sensitive to water and oxygen molecules. Hence, the samples were subjected to rigorous evacuation to remove any trace amounts of water and oxygen. The evacuation was hence done for as long as 36 h at 100 ± 5 °C. It seems possible that the discrepancy between this work and previous work[49] may be attributed to the more stringent evacuation conditions employed by us. In support of this, the photoyield of MV^+ was found to be about four times lower for samples evacuated for 12 h compared to 36 h.

Preliminary photoionization experiments were carried out with Cs−X zeolitic materials. $MV^{\bullet+}$ was not detected in samples that were not evacuated. ESR signals were 1 order of magnitude weaker in hydrated M−X zeolites compared to those that were dehydrated. The methyl viologen ion-exchanged Cs−X sample prior to irradiation was colorless and ESR silent. After being photoirradiated for a few minutes, it turned blue and showed a single symmetric ESR signal (Figure 2) at $g = 2.002$ with a peak-to-peak derivative line width of ∼20 G. The spectral widths of the ESR spectra are essentially the same as that of the methyl viologen cation radical in homogeneous solution at room temperature. This ESR signal and the blue color are typical of the $MV^{\bullet+}$ radical cation.[16,22,24] After being irradiated by 320 nm light at room temperature for up to 60 min, the samples showed strong ESR signals. Thus, there is a significant increase in the production of stable methyl viologen radicals. The background signals before irradiation were subtracted from the signals after irradiation to estimate the net photoyield. In addition, a visual change in the color of the Cs−$X/MV^{\bullet+}$ is easily discerned; the samples are colorless prior to irradiation but turn blue after irradiation, characteristic of $MV^{\bullet+}$ cation radicals. This further confirms the photoreduction of MV^{2+} into $MV^{\bullet+}$ cation radicals. The ESR signal and the blue color disappeared immediately when the sample tubes were exposed to air or oxygen. The photoproduced $MV^{\bullet+}$ radicals in the zeolite are thus unstable to trace amounts of air or oxygen.

Figures 3 and 4 show the changes in the intensity of the ESR signal due to $MV^{\bullet+}$ cation radicals in M−X zeolites. From Figure 3 we can see that the highest yield is obtained for Cs−

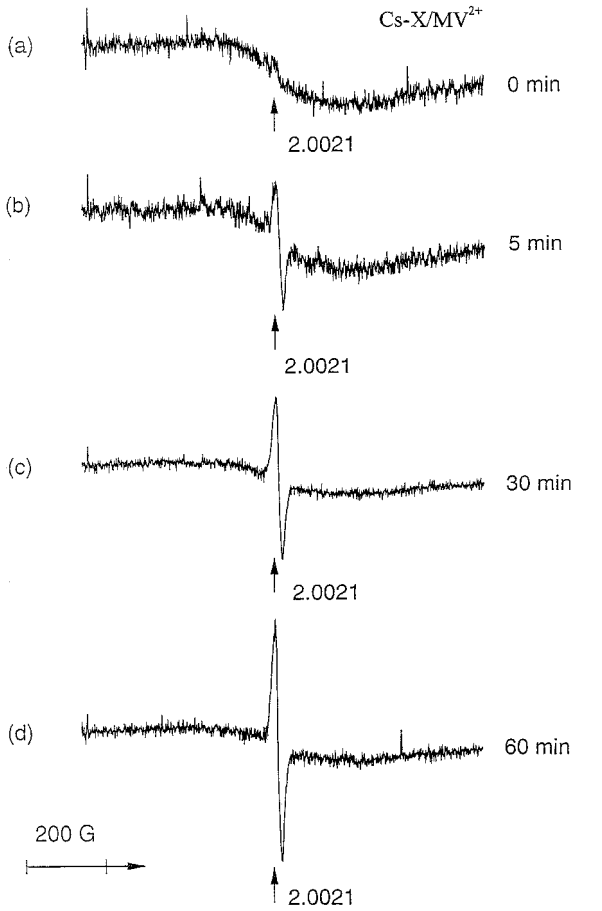

Figure 2. ESR spectra of Cs−X/MV^{2+} at room temperature upon UV irradiation at (a) 0 min, (b) 5 min, (c) 30 min, and (d) 60 min.

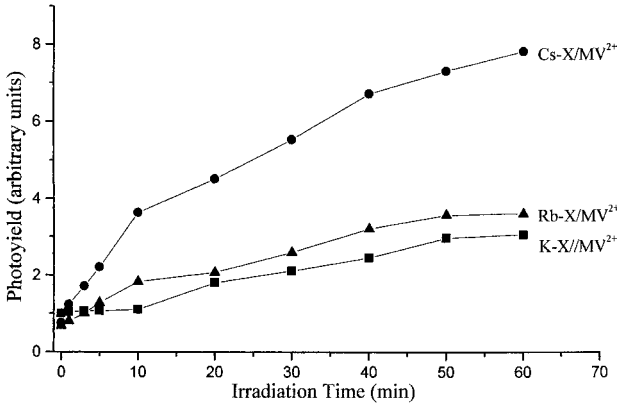

Figure 3. Room-temperature photoinduced methyl viologen radical cation yield measured by ESR versus irradiation time for M−X/MV^{2+} (M = Cs, Rb, K).

X/MV^+. Also, one can see that the ESR signals rapidly increase during the first 10 min of irradiation and then reach a plateau in about 60 min. An irradiation time of 60 min was selected for comparative photoyield and stability studies. The photoyield decreases in the order Cs−X > Rb−X > K−X > Na−X > Li−X. Thus, the nature of the exchanged metal ion in zeolite X plays an important role in stabilizing the photoproduced $MV^{\bullet+}$ cation radicals. For H−X there is only a small increase in the intensity of the ESR signal due to $MV^{\bullet+}$. After 30 min irradiation, the photoyield starts decreasing, the blue color of the sample starts fading, and the sample becomes colorless after 30 min standing in the dark. This suggests that the H−X zeolitic

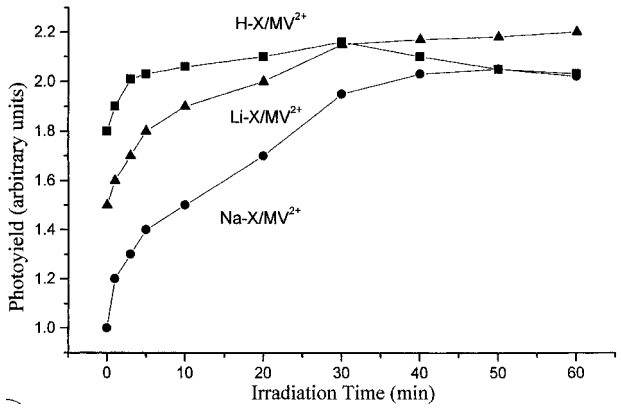

Figure 4. Room-temperature photoinduced methyl viologen radical cation yield measured by ESR versus irradiation time for M−X/MV^{2+} (M = Na, Li, H).

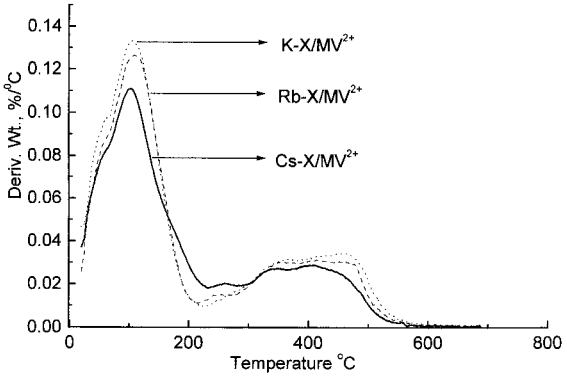

Figure 5. Differential thermal analysis of methyl viologen incorporated into Cs−X, Rb−X, and K−X zeolites.

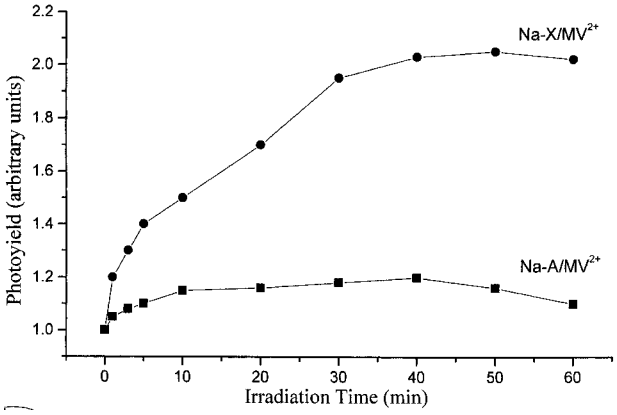

Figure 6. Room-temperature photoinduced methyl viologen radical cation yield measured by ESR versus irradiation time for Na−X/MV^{2+} and Na−A/MV^{2+}.

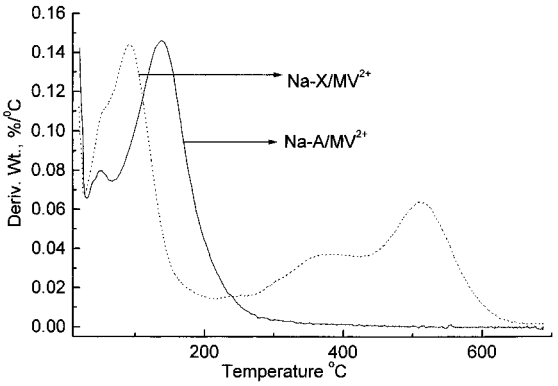

Figure 7. Differential thermal analysis of methyl viologen incorporated into Na−X and Na−A zeolites.

framework is unable to stabilize the photoproduced $MV^{\bullet+}$ due to its relatively high acidity compared to other M−X samples.

The rate of formation of the $MV^{\bullet+}$ cation radicals can be evaluated from the initial slopes in Figures 3 and 4 assuming first-order kinetics. The calculated rate constants for the formation of $MV^{\bullet+}$ are $k = 2.5 \times 10^{-1}$ s^{-1} for Cs−X, $k = 1.4 \times 10^{-1}$ s^{-1} for Rb−X, $k = 7.0 \times 10^{-2}$ s^{-1} for K−X, $k = 5.0 \times 10^{-2}$ s^{-1} for Na−X, and $k = 3.1 \times 10^{-2}$ s^{-1} for Li−X. This order of the rate constants is consistent with the order of the photoyields.

The stability of the photoproduced $MV^{\bullet+}$ radical is also an important factor in the design of efficient artificial photoredox systems. The stability of the $MV^{\bullet+}$ radicals was monitored by ESR spectroscopy. Among the alkali metal ion-exchanged zeolite X materials studied, Cs−X was found to exhibit the best stability. Assuming first-order kinetics, the half-lives ($t_{1/2}$) for the $MV^{\bullet+}$ decay are 63 days for Cs−X, 24 days for Rb−X, 20 days for K−X, 12 days for Na−X, and 10 days for Li−X. This order of the stabilities of the photoproduced $MV^{\bullet+}$ cation radicals is consistent with the order of the photoyields.

Figure 5 shows TGA results obtained from the incorporation of methyl viologen molecule into M−X zeolites. The curves show typically four weight losses. The first near 100 °C is attributed to water desorption, the second and third peaks near 250 and 350 °C are attributed to demethylation of MV^{2+},[50] and the fourth peak near 400 °C is assigned to the decomposition of methyl viologen in oxygen flow within the pores. The assignment of the 400 °C peak to decomposition of methyl viologen within the pores is supported by its absence when TGA is carried out in nitrogen flow. The TGA curves for Cs−X/MV^{2+}, Rb−X/MV^{2+}, and K−X/MV^{2+} are similar, indicating that the amount of methyl viologen incorporated inside the zeolite is similar. Thus we can conclude from the TGA experiments that methyl viologen does penetrate well into the pores of zeolite X.

The pore size of the host medium plays a significant role in the photoyield and the stability of the photoproduced $MV^{\bullet+}$ radical cations. Zeolite A is a small pore zeolite having a pore opening of 4.1 Å. The molecular dimensions of methyl viologen are 13.5 × 6.5 × 3.5 Å. Thus, zeolite A is probably not able to incorporate methyl viologen into its channels. Consequently, the photoyield of methyl viologen in zeolite A is expected to be quite low. The results obtained from the photoionization are shown in Figure 6. The photoyield in Na−A zeolite is found to be 2 times lower compared to Na−X zeolite. The adsorption of methyl viologen only on the external surface of Na−A zeolite can explain this small photoyield.

Figure 7 shows TGA results obtained from incorporation of methyl viologen into zeolites X and A. Na−X zeolite shows three weight losses. The first near 100 °C is attributed to water desorption, the second near 350 °C is attributed to demethylation of MV^{2+} and the third broad peak near 500 °C is assigned to the decomposition of methyl viologen within the pores. For zeolite A we see a weak peak near 100 °C attributed to water desorption and a second predominant peak at 150 °C attributed to methyl viologen desorption, but no peak near 500 °C. The lack of a peak near 500 °C indicates that methyl viologen does not penetrate into the pores of Na−A zeolite. The low photoyields in Na−A are consistent with the TGA interpretation.

Discussion

The ESR results clearly confirm the photoreduction of methyl viologen molecules into methyl viologen cation radicals in alkali metal ion-exchanged zeolites at room temperature. The increase in the intensity of the ESR signal due to the $MV^{\bullet+}$ radical cations with time in the case of M−X samples (Figure 3) suggests that the alkali metal ion-exchanged zeolites assist in the formation and stabilization of the photoproduced methyl viologen cation radical. However, the photoyield depends on the nature of the alkali metal ion-exchanged into the zeolite framework.

Experiments with different alkali metal ions in $M-X/MV^{2+}$ samples show strong ESR signals at room temperature. Figures 3 and 4 show an increase in the intensity of the ESR signal due to $MV^{\bullet+}$ with irradiation time for M−X with alkali metal ions in ion-exchange sites. As one can observe from Figure 3, the presence of Cs^+ in zeolite X enhances the photoyield compared to other alkali metal ions such as Rb^+, K^+, Na^+, or Li^+. The photoionization efficiency for MV^{2+} in M−X zeolites decreases in the order $Cs-X/MV^{2+} > Rb-X/MV^{2+} > K-X/MV^{2+} > Na-X/MV^{2+} > Li-X/MV^{2+} > H-X/MV^{2+}$. Thus the photoreduction efficiency can be controlled by the nature of the metal ion in the ion-exchange sites. TGA results (Figure 5) clearly show that the amount of methyl viologen incorporated in different M−X zeolites is similar, suggesting that the difference obtained in the photoyield is due to other factors such as the electron donor strength of the zeolite framework.

The cations in the zeolites, in addition to compensating the negative charges in the framework, also govern the electron donor strength of the zeolite framework. The electron donor strength or basicity of the framework has been demonstrated to increase upon increasing the electropositivity of the cation.[18,30,31,43] Thus the electron donor strength of zeolites increases in the order Li−X < Na−X < K−X < Rb−X < Cs−X. To directly calculate the electron donor strength of the zeolite framework, it is necessary to have the effective ionization potential of the zeolite framework $I_p(Z)$. However, values of $I_p(Z)$ are not known for solid zeolite X although $I_p(Z)$ has been estimated to be 11.4 eV for Na−ZSM-5.[53]

Sanderson's electronegativity equalization principle has served as a theoretical basis to correlate the experimentally observed electron donor strength of the framework and the partial charge of the framework oxygens.[38] We use Sanderson's partial charges of the framework oxygen atoms as a measure for the framework electron donor strength since they have been shown to be linearly correlated with the experimentally observed framework electron donor strengths. Sanderson's partial charges of the framework oxygen atoms for the MV^{2+}-doped X zeolites were calculated on the basis of the chemical compositions listed in Table 1. Sanderson's electronegativity S_z of each alkali metal ion-exchanged zeolite was calculated according to

$$S_z = (S_M{}^a S_{Si}{}^b S_{Al}{}^c S_O{}^d)^{1/(a+b+c+d)} \quad (1)$$

where S_M, S_{Si}, S_{Al}, and S_O represent Sanderson's electronegativities of the alkali metal cation, silicon, aluminum, and oxygen, respectively, and a, b, c, and d represent the numbers of the corresponding element in a unit cell. Sanderson's partial charge of the framework (δ_O) was obtained from

$$\delta_O = (S_z - S_O)/2.08 S_O{}^{1/2} \quad (2)$$

The perturbation of the partial charges caused by the replacement of two alkali metal ions with one MV^{2+} was neglected. The values of Sanderson's electronegativity for each element Si, Al, O, Li, Na, K, Rb, and Cs were taken from the literature.[54]

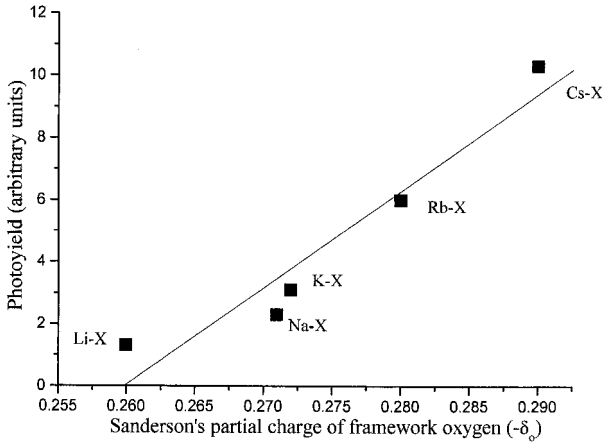

Figure 8. Relationship between photoyield and the calculated Sanderson's partial charge of the framework oxygen of M−X (M = Cs, Rb, K, Na, Li).

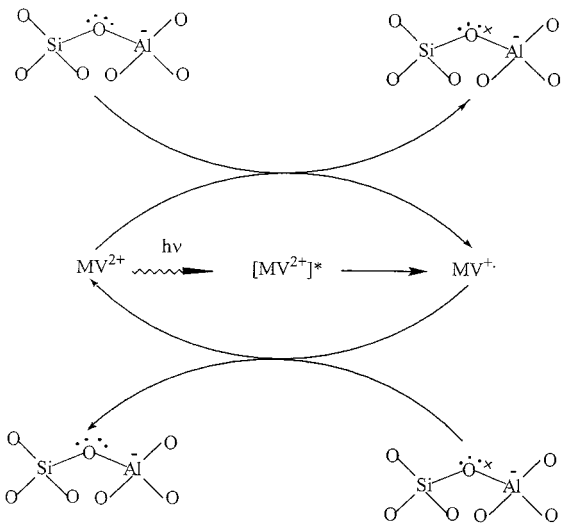

Figure 9. Possible mechanism for the photoreduction of MV^{2+} in M−X zeolites (M = Cs, Rb, K, Na, Li).

Figure 8 shows the relationship obtained between the photoyield and the calculated Sanderson's partial charge of the framework oxygens. An excellent linear relationship is obtained that leads us to conclude that the yield of the photoproduced $MV^{\bullet+}$ increases with an increase in the negative charge density of the framework oxygens, that is, upon increasing the framework electron donor strength or basicity. The fact that the photoyield and the stability of photoproduced $MV^{\bullet+}$ decrease in the order $Cs-X/MV^{2+} > Rb-X/MV^{2+} > K-X/MV^{2+} > Na-X/MV^{2+} > Li-X/MV^{2+}$ clearly indicate that not only the single electron-transfer step to form $MV^{\bullet+}$ but also the $MV^{\bullet+}$ stability or decay dynamics are dependent on the electron donor nature of the cation. A possible explanation is that the major pathway for the decay of the photoproduced $MV^{\bullet+}$ cation radical is back electron transfer from $MV^{\bullet+}$ to a radical center in the zeolite to regenerate MV^{2+} in its ground state and an oxygen lone pair in the framework. A possible schematic mechanism of the processes occurring is depicted in Figure 9. Irradiation of light in $M-X/MV^{2+}$ causes the excitation of MV^{2+}. In its excited state, MV^{2+} abstracts one electron from an oxygen of the zeolite framework, giving rise to an oxygen radical center and $MV^{\bullet+}$. The stability of the photoproduced $MV^{\bullet+}$ then

depends on the electron density of the oxygen acting as the electron donor. The higher the electron density on the oxygen acting as the electron donor, the slower the rate of back electron transfer. Hence the stability of $MV^{\bullet+}$ in a series of zeolites follows the same order as their basicity, i.e., Cs−X > Rb−X > K−X > Na−X > Li−X. Thus the electron donor sites seem to be oxygens of the zeolite framework.

Conclusions

Microporous alkali metal ion containing zeolite X show stable photoinduced charge separation of methyl viologen molecules. The $MV^{\bullet+}$ cation radical photoyield depends on the electron donor strength or basicity of the zeolite as determined by its metal cation. The photoyields for a series of alkali metal containing zeolite X materials can be linearly correlated with Sanderson's partial charges on the framework oxygens. The electron donor sites are believed to be oxygen sites in the framework. The $MV^{\bullet+}$ photoyield is dependent on the basicity and the pore size of the zeolite. The results clearly indicate that Cs−X zeolites provide the most appropriate steric and electrostatic environment to retard back electron transfer and increase the lifetime of photogenerated radical ions from methyl viologen for many days at room temperature.

Acknowledgment. This research was supported by the Chemical Sciences, Geosciences, and Biosciences Division, Office of the Basic Energy Sciences, U.S. Department of Energy, the Texas Advanced Research Program and the Environmental Institute of Houston.

References and Notes

(1) Gust, D.; Moore, T. A.; Moore, A. L. *Acc. Chem. Res.* **2001**, *34*, 40.
(2) Scaiano, J. C.; Garcia, H. *Acc. Chem. Res.* **1999**, *32*, 783.
(3) Meyer, T. J. *Acc. Chem. Res.* **1989**, *26*, 198.
(4) Infelta, P. P.; Grätzel, M.; Fendler, J. H. *J. Am. Chem. Soc.* **1980**, *102*, 1479.
(5) Hurst, J. K.; Lee, L. Y. C.; Grätzel, M. *J. Am. Chem. Soc.* **1983**, *105*, 7048.
(6) Lanot, M. P.; Kevan, L. *J. Phys. Chem.* **1991**, *95*, 10178.
(7) Xiang, B.; Kevan, L. *Colloid Surf. A* **1993**, *72*, 11.
(8) Xiang, B.; Kevan, L. *Langmuir* **1995**, *11*, 860.
(9) Xiang, B.; Kevan, L. *J. Phys. Chem.* **1994**, *98*, 5120.
(10) Sung-Suh, H. M.; Kevan, L. *J. Chem. Soc., Faraday Trans*. **1998**, *94*, 1417.
(11) Krueger, J. S.; Mayer, J. E.; Mallouk, T. E. *J. Am. Chem. Soc.* **1988**, *110*, 8232.
(12) Vermeulen, L. A.; Thompson, M. E. *Nature* **1992**, *358*, 656.
(13) Slama-Schwok, A.; Avnir, D.; Ottolenghi, M. *Nature* **1992**, *355*, 240.
(14) Persaud, L.; Bard, A. J.; Campion, A.; Fox, M. A.; Mallouk, T. E.; Webber, S. E.; White, J. M. *J. Am. Chem. Soc.* **1987**, *109*, 7309.
(15) Wolszczak, M.; Stradowski, Cz. *Radiat. Phys. Chem*. **1989**, *3*, 355.
(16) Bockman, T. M.; Kochi, J. K. *J. Org. Chem*. **1990**, *55*, 4127.
(17) Watanabe, T.; Honda, K. *J. Phys. Chem*. **1982**, *86*, 2617.
(18) Wheeler, J.; Thomas, J. K. *J. Phys. Chem*. **1982**, *86*, 4540.
(19) McManus, H. J. D.; Kevan, L. *J. Phys. Chem*. **1991**, *95*, 5996.
(20) Dutta, P. K.; Turbeville, W. *J. Phys. Chem*. **1992**, *96*, 9410.
(21) Lukac, S.; Harbour, J. R. *J. Am. Chem. Soc.* **1983**, *105*, 4248.
(22) Colaneri, M. J.; Kevan, L.; Schmehl, R. *J. Phys. Chem.* **1989**, *93*, 397.
(23) Colaneri, M. J.; Kevan, L.; Thompson, D. H. P.; Hurst, J. K. *J. Phys. Chem.* **1987**, *91*, 4072.
(24) Yoon K. B.; Kochi, J. K. *J. Am. Chem. Soc.* **1988**, *110*, 6586.
(25) Yoon K. B.; Kochi, J. K. *J. Am. Chem. Soc.* **1989**, *111*, 1128.
(26) Sankararaman, S.; Yoon K. B.; Yabe, T.; Kochi, J. K. *J. Am. Chem. Soc.* **1991**, *113*, 1419.
(27) Barrer, R. M. *Zeolites and Clay Minerals as Sorbents and Molecular Sieves*; Academic Press: London, 1978.
(28) van Bekkum, H., Flanigen, E. M., Jansen, J. C., Eds. *Introduction to Zeolite Science and Practice*; Elsevier: Amsterdam, 1991.
(29) Rabo, J. A.; Angell, C. L.; Kasai, P. H.; Schomaker, V. *Discuss. Faraday Soc*. **1966**, *41*, 328.
(30) Mortier, W. J. *J. Catal*. **1978**, *55*, 138.
(31) Barr, T. L.; Lishka, M. A. *J. Am. Chem. Soc*. **1986**, *108*, 3178.
(32) Ono, Y. *Stud. Surf. Sci. Catal.* **1980**, *5*, 19.
(33) Mochida, I.; Yoneda, Y. *J. Org. Chem*. **1968**, *33*, 2161.
(34) Hattori, H. *Chem. Rev*. **1995**, *95*, 537.
(35) Kaushik, V. K.; Bhat, S. G. T.; Corbin, D. R. *Zeolites* **1993**, *13*, 671.
(36) Mortier, W. J.; Schoonheydt, R. A. *Prog. Solid State Chem*. **1985**, *16*, 1.
(37) Huang, M.; Adnot, A.; Kaliaguine, S. *J. Am. Chem. Soc.* **1992**, *114*, 10005.
(38) Choi, S. Y.; Park, Y. S.; Hong, S. B.; Yoon, K. B. *J. Am. Chem. Soc.* **1996**, *118*, 9377.
(39) Tanabe, K.; Misono, M.; Ono, Y.; Hattori, H. *Stud. Surf. Sci. Catal.* **1989**, *51*, 1.
(40) Okamoto, Y.; Ogawa, M.; Maezawa, A.; Imanaka, T. *J. Catal.* **1988**, *112*, 427.
(41) Yashima, T.; Sato, K.; Hayasaka, T.; Hara, N. *J. Catal*. **1972**, *26*, 303.
(42) Barthomeuf, D.; Ha, B.-H. *J. Chem. Soc., Faraday Trans.* **1973**, *69*, 2173.
(43) Uytterhoeven, L.; Dompas, D.; Mortier, W. J. *J. Chem. Soc., Faraday Trans.* **1992**, *88*, 2753.
(44) Barr, T. L. *Zeolites* **1990**, *10*, 760.
(45) Mirodatos, C.; Pichat, P.; Barthomeuf, D. *J. Phys. Chem.* **1976**, *80*, 1335.
(46) Corma, A.; Fornes, V.; Garcia, H.; Marti, M. A. *Chem. Mater.* **1995**, *7*, 2136.
(47) Chen, F. R.; Fripiat, J. J. *J. Phys. Chem.* **1992**, *96*, 819.
(48) Rhodes, C. J. *J. Chem. Soc., Faraday Trans.* **1991**, *87*, 3179.
(49) McManus, H. J. D.; Finel. C.; Kevan, L. *Radiat. Phys. Chem*. **1995**, *45*, 761.
(50) Alvaro, M.; Garcia, H.; Garcia, S.; Marquez, F.; Scaiano, J. C. *J. Phys. Chem. B* **1997**, *101*, 3043.
(51) Park, Y. S.; Um, S. Y.; Yoon, K. B. *J. Am. Chem. Soc.* **1999**, *121*, 3193.
(52) Baldovi, M. F.; Cozens, F. L.; Fornes, V.; Garcia, H.; Scaiano, J. C. *Chem. Mater*. **1996**, *8*, 152.
(53) Werst, D. W.; Tartakovsky, E. E.; Piocos, E. A.; Trifunac, A. D. *J. Phys. Chem. B* **1994**, *98*, 10249.
(54) Huheey, J. E.; Keiter, E. A.; Keiter, R. L. *Inorganic Chemistry*, 4th ed.; Harper Collins College Publications: New York, 1993; p 187.